

Transcriptomic profiling of human corneal epithelial cells exposed to PM_{2.5}: Identification of differentially expressed genes and pathways

Yingchao Li^{1,A,B}, Wenjing Liu^{1,B,C}, Huijing Bao^{1,C,D}, *Yibin Ma^{1,E,F}, *Han Zhang^{2,D,E}

¹ Department of Ophthalmology, The Affiliated Taian City Central Hospital of Qingdao University, China

² Department of Ophthalmology, Shandong Provincial Hospital Affiliated to Shandong First Medical University, Jinan, China

A – research concept and design; B – collection and/or assembly of data; C – data analysis and interpretation;

D – writing the article; E – critical revision of the article; F – final approval of the article

Advances in Clinical and Experimental Medicine, ISSN 1899–5276 (print), ISSN 2451–2680 (online)

Adv Clin Exp Med. 2026

Address for correspondence

Yibin Ma

E-mail: mybzlj@163.com

Funding sources

This work was supported by the Natural Science Foundation of Shandong Province (grant No. ZR2022LSW011) and the Taian City Science and Technology Innovation Development Project (grants No. 2021NS207, 2022NS203, and 2023NS273).

Conflict of interest

None declared

Acknowledgements

The authors thank Prof. Qing-Jun Zhou of Shandong Eye Institute, Shandong First Medical University and Shandong Academy of Medical Sciences for providing HCECs.

*Yibin Ma and Han Zhang contributed equally to this work.

Received on April 21, 2025

Reviewed on June 24, 2025

Accepted on July 3, 2025

Published online on February 24, 2026

Cite as

Li Y, Liu W, Bao H, Ma Y, Zhang H. Transcriptomic profiling of human corneal epithelial cells exposed to PM_{2.5}: Identification of differentially expressed genes and pathways [published online as ahead of print on February 24, 2026]. *Adv Clin Exp Med*. 2026. doi:10.17219/acem/207872

DOI

10.17219/acem/207872

Copyright

Copyright by Author(s)

This is an article distributed under the terms of the Creative Commons Attribution 3.0 Unported (CC BY 3.0) (<https://creativecommons.org/licenses/by/3.0/>)

Abstract

Background. High levels of PM_{2.5} air pollution pose serious health risks, especially in rapidly urbanizing areas. While its effects on organs such as the heart and lungs are well documented, its effects on the cornea remain less well understood. Emerging evidence links PM_{2.5} exposure to corneal damage through processes such as autophagy, inflammation, and oxidative stress; however, the precise molecular pathways remain largely unknown.

Objectives. This study aimed to identify key genes and signaling pathways in PM_{2.5}-exposed human corneal epithelial cells (HCECs) using RNA sequencing and bioinformatics analysis.

Materials and methods. Human corneal epithelial cells were cultured and exposed to 25 µg/mL PM_{2.5} for 24 h. High-throughput sequencing was performed after total RNA extraction and library construction for mRNA and microRNA (miRNA). Clean reads were mapped to the reference genome after filtering out low-quality reads. The Differential Expression Sequencing 2 (DESeq2) R package was used to identify differentially expressed (DE) mRNAs and miRNAs with a fold change ≥ 2 or ≤ 0.5 and a false discovery rate (FDR) ≤ 0.001 . Bioinformatics analyses included hierarchical clustering, protein–protein interaction network construction, target gene prediction, and Gene Ontology (GO) and Kyoto Encyclopedia of Genes and Genomes (KEGG) pathway enrichment.

Results. The analysis identified 45 DE mRNAs, including 14 upregulated and 31 downregulated transcripts, along with 16 upregulated miRNAs. A gene interaction network was constructed comprising nine mRNAs (6 upregulated and 3 downregulated), while a combined miRNA–mRNA network included 14 miRNAs and 21 mRNAs, forming 73 interaction pairs. Functional enrichment analysis of these genes revealed 30 significantly enriched GO terms, as well as 27 KEGG signaling pathways.

Conclusions. This study constructed regulatory networks and identified genes DE in the corneal response to PM_{2.5} exposure, particularly those involved in autophagy, inflammatory responses, and oxidative stress–related pathways. These results lay the groundwork for further research into the effects of PM_{2.5} on ocular surface health and provide insights into the molecular mechanisms underlying PM_{2.5}-induced damage to human corneal epithelial cells, potentially guiding the development of targeted diagnostics or therapies to mitigate ocular surface injury caused by PM_{2.5}.

Key words: PM_{2.5}, bioinformatics analysis, human corneal epithelial cells

Highlights

- Forty-five mRNAs and 16 microRNAs were differentially expressed in human corneal epithelial cells following PM_{2.5} exposure.
- Gene and microRNA–mRNA interaction networks were constructed to elucidate the regulatory mechanisms underlying PM_{2.5}-induced corneal damage.
- Functional enrichment analysis identified 30 Gene Ontology terms and 27 Kyoto Encyclopedia of Genes and Genomes pathways associated with inflammation, cellular stress, and immune responses.
- These findings provide novel insights into the molecular effects of air pollution on ocular surface health.
- The results may inform future therapeutic strategies for pollution-related corneal disorders.

Background

Air pollution is a well-established global public health concern.¹ Among its various components, fine particulate matter (PM_{2.5}) is considered particularly hazardous.^{2,3} In developing nations undergoing rapid industrialization and urban expansion, such as China, PM_{2.5} levels have reached critical thresholds; for instance, the annual average PM_{2.5} concentration in eastern China exceeded 80 µg/m³ in 2010.^{4,5} Exposure to PM_{2.5} has been widely linked to elevated risks of cancer, respiratory and cardiovascular diseases, and increased mortality.^{6–10}

Despite these findings, its effects on the ocular surface, particularly the cornea, which is directly exposed to airborne pollutants, have received less attention. Xiang et al. emphasized the harmful effects of PM_{2.5} on ocular health.¹¹ Recent studies have suggested that PM_{2.5} may contribute to corneal epithelial damage through mechanisms such as oxidative stress, autophagy dysregulation, and pro-inflammatory responses.^{12–16} However, the precise molecular mechanisms involved in these corneal responses remain largely unknown, and whether they mirror those observed in other organs is still unclear.

Objectives

Through comprehensive bioinformatics analysis, this study aims to clarify the key genes and signaling pathways implicated in the effects of PM_{2.5} on the cornea.

Materials and methods

Culture and exposure of human corneal epithelial cells to PM_{2.5}

Human corneal epithelial cells (HCECs) were provided by the Shandong Eye Institute, Shandong Provincial Key Laboratory of Ophthalmology, Qingdao, China. The cells were cultured in Dulbecco's modified Eagle's medium (DMEM)/Ham's F12 medium supplemented

with 1% penicillin–streptomycin and 10% fetal bovine serum (FBS). The medium was changed every 2 days, and the cultures were maintained at 37°C in an atmosphere containing 5% CO₂.^{17–19} Cells were seeded in 6-well plates and cultured for 24–48 h in regular growth medium. The cells were then rinsed with phosphate-buffered saline (PBS) and incubated for 24 h in either control medium or a PM_{2.5} solution at a concentration of 25 µg/mL. The PM_{2.5} used was SRM 1648a (National Institute of Standards and Technology (NIST), Gaithersburg, USA), which was suspended in sterile PBS and sonicated for 30 min in a water-bath sonicator (US-220; Zhongke Scientific Instrument, Beijing, China) to ensure even dispersion before application. Each treatment was replicated 3 times for subsequent RNA extraction. Three biological replicates were used for both mRNA and miRNA sequencing analyses. The cells used for all experiments were between passages 2 and 5. The PM_{2.5} employed was the urban particulate matter reference standard (SRM 1648a), sourced from the NIST and representative of urban environments.

This study did not involve any human participants or animal experiments. Only commercially available human corneal epithelial cell lines were used. Therefore, ethical approval was not required.

Library preparation

RNA library preparation

Total RNA from 2 distinct groups was qualified and quantified using a bioanalyzer (Agilent 2100 Bioanalyzer; Agilent Technologies, Santa Clara, USA) before being randomly fragmented. These fragments then served as templates for 1st-strand cDNA synthesis, followed by 2nd-strand synthesis. The fragments were then purified using the QIAquick polymerase chain reaction (PCR) kit (Qiagen, Hilden, Germany), eluted with elution buffer, end-repaired, adenylated by the addition of a single 'A' base, and ligated to sequencing adapters. The uracil-N-glycosylase (UNG) enzyme (Thermo Fisher Scientific, Waltham, USA) was then used to degrade the 2nd strand. Following fragment

size selection by agarose gel electrophoresis, polymerase chain reaction (PCR) amplification was performed to generate the sequencing library.

microRNA library preparation

RNA concentrations in 6 samples were determined using a bioanalyzer (Agilent 2100 Bioanalyzer; Agilent Technologies). RNAs of different fragment sizes were separated by sodium dodecyl sulfate–polyacrylamide gel electrophoresis (SDS–PAGE), and bands ranging from 18 to 30 nucleotides were excised to recover small RNAs. According to the manufacturer's instructions for T4 RNA ligase (Thermo Fisher Scientific), these RNAs were ligated to 5' and 3' adapters before being reverse-transcribed into cDNA molecules. To complete library construction, the PCR products were purified by PAGE and dissolved in ethidium bromide (EB) solution.

RNA-seq method

Raw sequencing reads were subjected to quality control using FastQC v. 0.11.9 (<https://www.bioinformatics.babraham.ac.uk/projects/fastqc/>) to evaluate metrics such as per-base sequence quality, GC content (the molar ratio of guanine + cytosine bases in DNA), and adapter contamination. Trimmomatic v. 0.39²⁰ (<http://www.usadellab.org/cms/?page=trimmomatic>) was employed to remove adapter sequences and low-quality bases, using parameters: ILLUMINACLIP:2:30:10, SLIDINGWINDOW:4:20, and MINLEN:36. Cleaned reads were aligned to the human reference genome (GRCh38/hg38) using HISAT2 v. 2.2.1 (<https://daehwankimlab.github.io/hisat2/>),²¹ a splice-aware aligner. The resulting files of sequence alignment map (SAM) were converted to sorted binary alignment map (BAM) files using SAMtools v. 1.10 (<https://www.htslib.org/doc/1.10/samtools.html>).²² Subsequently, transcript assembly and quantification were performed with StringTie v. 2.2.1 (<https://ccb.jhu.edu/software/stringtie/>).²³ For each sample, transcript abundance was calculated based on the reference gene annotation (GTF) file, and novel transcript isoforms were also predicted. Expression levels were quantified in fragments per kilobase of transcript per million mapped reads (FPKM). Gene-level count matrices were generated using the prepDE.py script provided with StringTie. Differential gene expression analysis was conducted using the DESeq2²⁴ package v. 1.38.3 in R v. 4.2.2 (R Foundation for Statistical Computing, Vienna, Austria). Raw count data were normalized, and statistical testing was performed using the Wald test with Benjamini–Hochberg correction for multiple comparisons. Genes with an adjusted $p < 0.050$ and $|\log_2 \text{fold change}| \geq 1$ were considered significantly differentially expressed (DE). To interpret the biological significance of the DE genes, Gene Ontology (GO) enrichment and Kyoto Encyclopedia of Genes and Genomes (KEGG) pathway analyses were performed

using the clusterProfiler²⁵ package (v. 4.6.2) in R. Enrichment results were visualized with dot plots and pathway diagrams to identify biological processes and signaling pathways significantly associated with DE genes.

Results

Analysis of 6 samples from both the PM_{2.5} group and the negative control group revealed 45 DE mRNAs (Fig. 1A and Supplementary Table 1), including 14 up-regulated and 31 downregulated transcripts. Similarly, analysis of the same sample set identified 16 DE miRNAs, all of which were upregulated (Fig. 1B, Supplementary Table 2). Using Cytoscape software (URL: <https://cytoscape.org/>), an interaction network of DE mRNAs was constructed, comprising 9 nodes and 7 edges (Fig. 2). This network included 6 upregulated and 3 downregulated genes. These 9 mRNAs were selected for downstream analysis based on their centrality and connectivity within the protein–protein interaction (PPI) network, indicating potential roles as regulatory hubs.

The interaction network included 35 DE genes, consisting of 14 miRNAs and 21 mRNAs, with 73 interaction pairs identified (Fig. 3). Key genes in the miRNA–mRNA network were selected based on overlap in target prediction, consistency of differential expression, and biological relevance to pathways identified through enrichment analysis.

Functional enrichment analysis was performed on the 9 DE mRNAs from the network, revealing enrichment in 30 GO terms, segmented into 3 categories: biological process (BP), cellular component (CC), and molecular function (MF). The top 10 entries from each category are shown in Fig. 4 and Supplementary Table 3. Additionally, 27 signaling pathways were identified through KEGG analysis. The top 20 entries from each category are shown in Fig. 5 and Supplementary Table 4.

Discussion

PM_{2.5} is a complex mixture consisting of various sources, such as automobile exhaust, combustion smoke, soil, and cooking fumes. Its constituents include metals, salts, volatile organic compounds, hydrocarbons, and endotoxins.²⁶ Owing to this intricate composition, the impact of PM_{2.5} on human health is multifaceted. However, its ocular effects, particularly on the cornea, remain understudied. This study aims to explore the influence of PM_{2.5} on the cornea and to identify key genes and signaling pathways involved.

We identified several novel genes and miRNA candidates not previously associated with PM_{2.5}-induced ocular damage. Our study found that several genes in HCECs exhibited differential expression after exposure to PM_{2.5}.

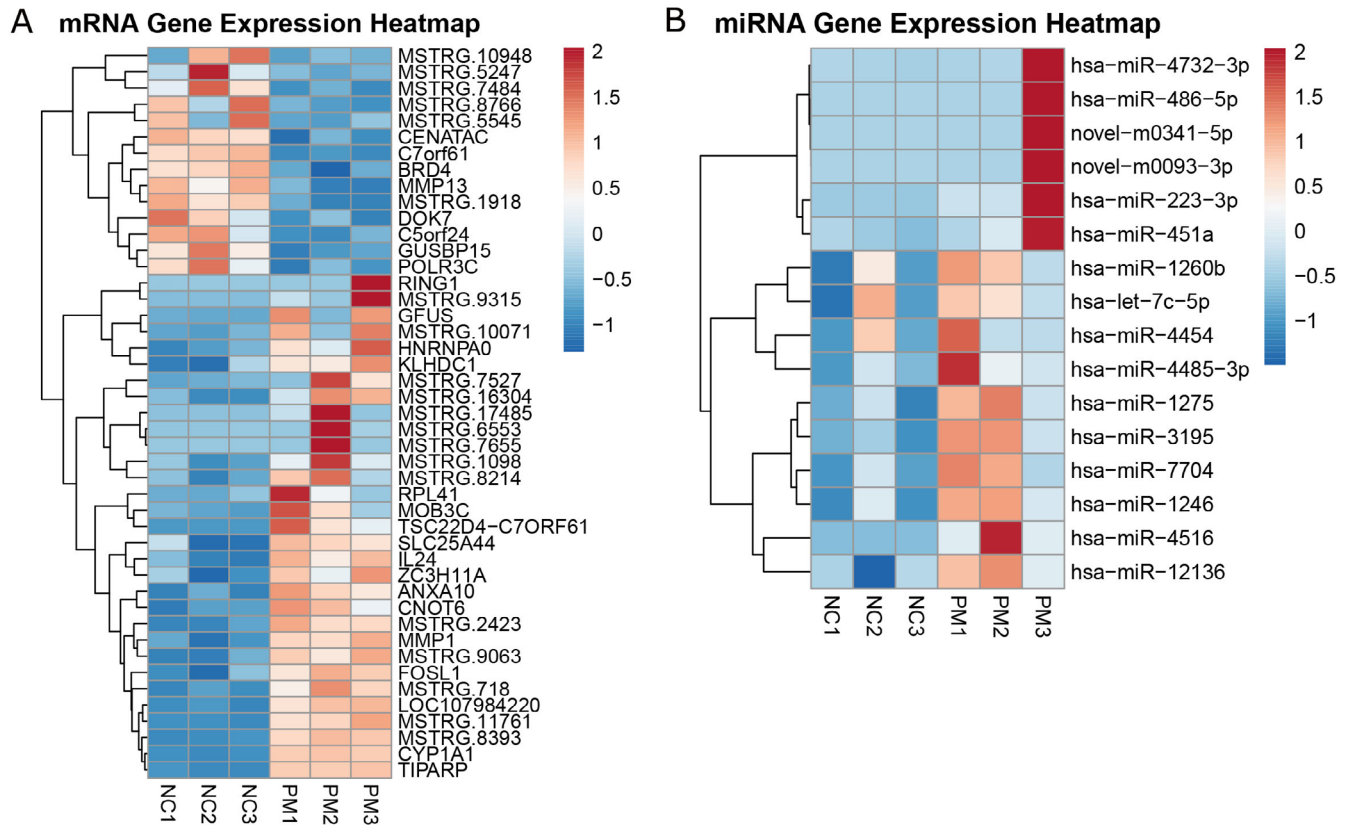


Fig. 1. Heatmap of differentially expressed (DE) genes. A: Heat map of DE mRNAs; B: Heat map of DE miRNAs

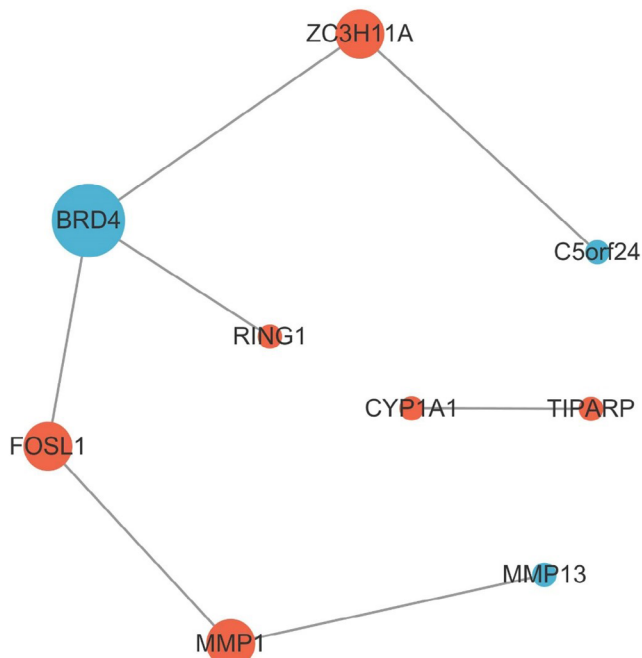


Fig. 2. Interaction network of differentially expressed (DE) mRNAs. Red points represent upregulated genes; blue points indicate downregulated genes. The size of each point correlates with the p-value

These include *BRD4*, *FOSL1*, and *CYP1A1*, which appear to play central roles in regulating oxidative stress, autophagy, and inflammation in the corneal epithelium. *BRD4*, a member of the bromodomain and extraterminal protein

family, recognizes and binds to acetylated lysine residues on histone tails.²⁷ It is implicated in the regulation of various inflammatory cytokines, including interleukin (IL)-1 β , IL-6, IL-8, and IL-9, and functions as a transcriptional regulator that modulates autophagy and oxidative stress via lysosomal pathways.^{28–30}

FOSL1, a component of the AP-1 transcription factor complex, has been reported to be upregulated following PM_{2.5} exposure in lung epithelial cells and may contribute to autophagy inhibition, inflammation, and oxidative stress.^{31,32} Studies have suggested that *FOSL1* can promote apoptosis and inflammation through the AMPK signaling pathway,³³ and that its inhibition leads to reduced pro-inflammatory cytokine expression.^{34,35} *FOSL1* also interacts with the Nrf2 pathway, a key regulator of oxidative stress.^{36–38}

Cytochrome P450 enzymes (CYPs) are essential for the metabolism of various substances, including heavy metals and drugs.³⁹ *CYP1A1*, a cytochrome P450 enzyme, has been shown to be upregulated in corneal epithelial cells following exposure to airborne pollutants such as cigarette smoke and house dust.^{11,40} It participates in xenobiotic metabolism and is regulated by the aryl hydrocarbon receptor (AhR) signaling pathway.^{39–45} Suppression of *CYP1A1* has been linked to reduced reactive oxygen species (ROS) production and oxidative stress.⁴⁵ Its co-regulation with *TIPARP* via AhR signaling underscores its potential importance in pollutant-induced ocular responses

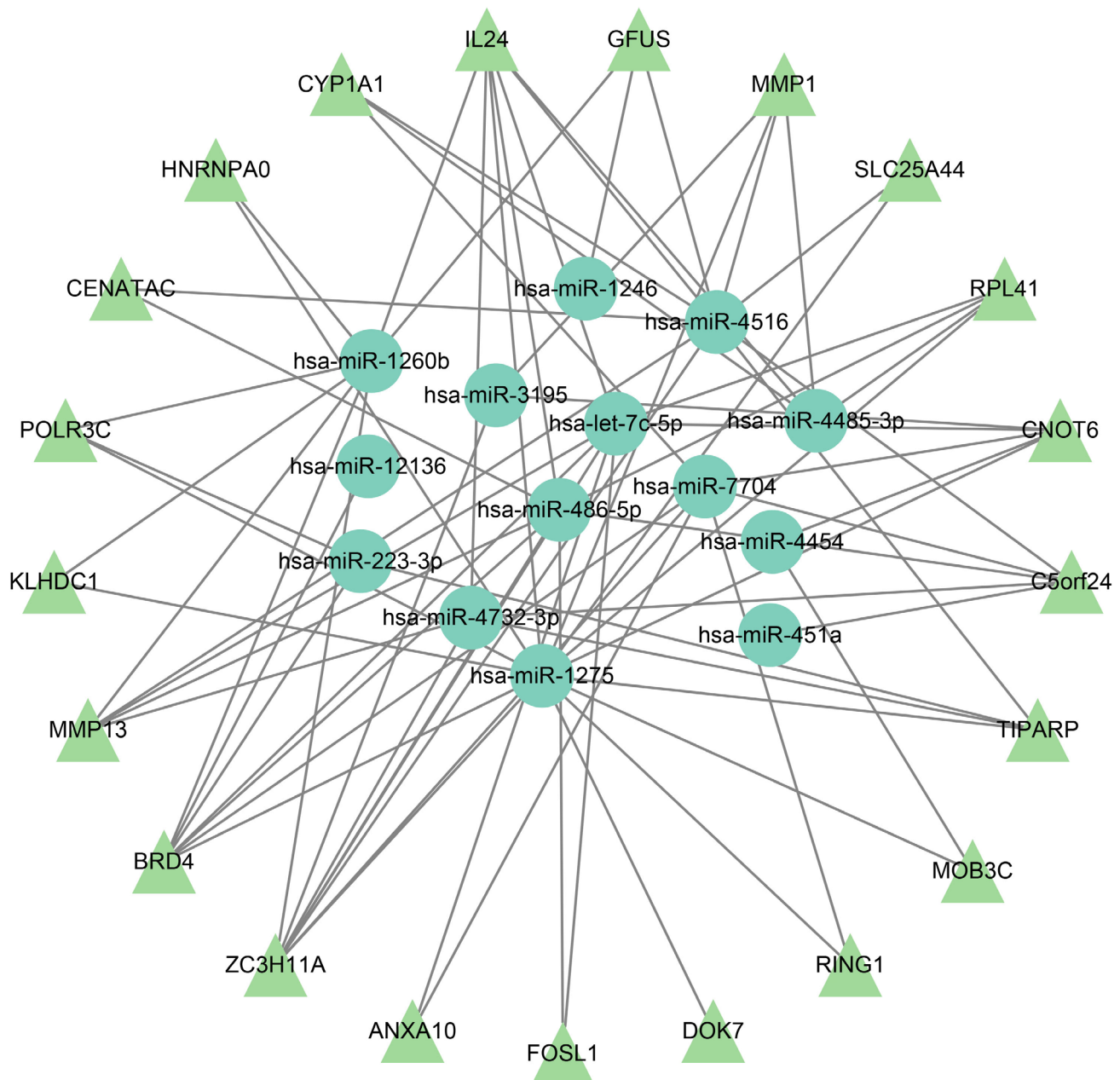


Fig. 3. miRNA-mRNA regulation network, consisting of 35 nodes and 73 edges. Triangles represent mRNAs and circles denote miRNAs

– In addition, we identified 16 DE miRNAs. Among these, several novel miRNA–mRNA interactions potentially relevant to corneal responses to PM_{2.5} were identified:

– miR-1275, predicted to target BRD4 and TIPARP, may regulate autophagy and ROS generation and inflammation when inhibited.^{46–48}

– miR-223-3p, also targeting BRD4 and TIPARP, has been linked to the modulation of autophagy and oxidative stress in both ocular and systemic contexts.^{49–52}

– miR-486-5p, targeting BRD4 and FOSL1, was shown to induce autophagy upon inhibition and reduce inflammation and oxidative damage.^{53–55}

– miR-4516, associated with CYP1A1 and TIPARP, may regulate autophagic responses to metal components in PM.⁵⁶

– miR-4454 expression is elevated in PM-exposed populations, although its ocular mechanism is unclear.⁵⁷

– let-7c-5p, which may regulate BRD4 and FOSL1, has been implicated in abnormal autophagy in lens epithelial cells.⁵⁸

Gene Ontology analysis and KEGG signaling pathway enrichment were performed for the DE mRNAs. The enriched BP terms were mainly related to nitrogen compound metabolic processes and primary metabolic processes. The enriched CC terms were primarily associated with the nucleoplasm, extracellular matrix (ECM), and mitochondrial membrane. The enriched MF terms were mainly related to enzyme activation or binding, such as metalloendopeptidase activity, metallopeptidase activity, and

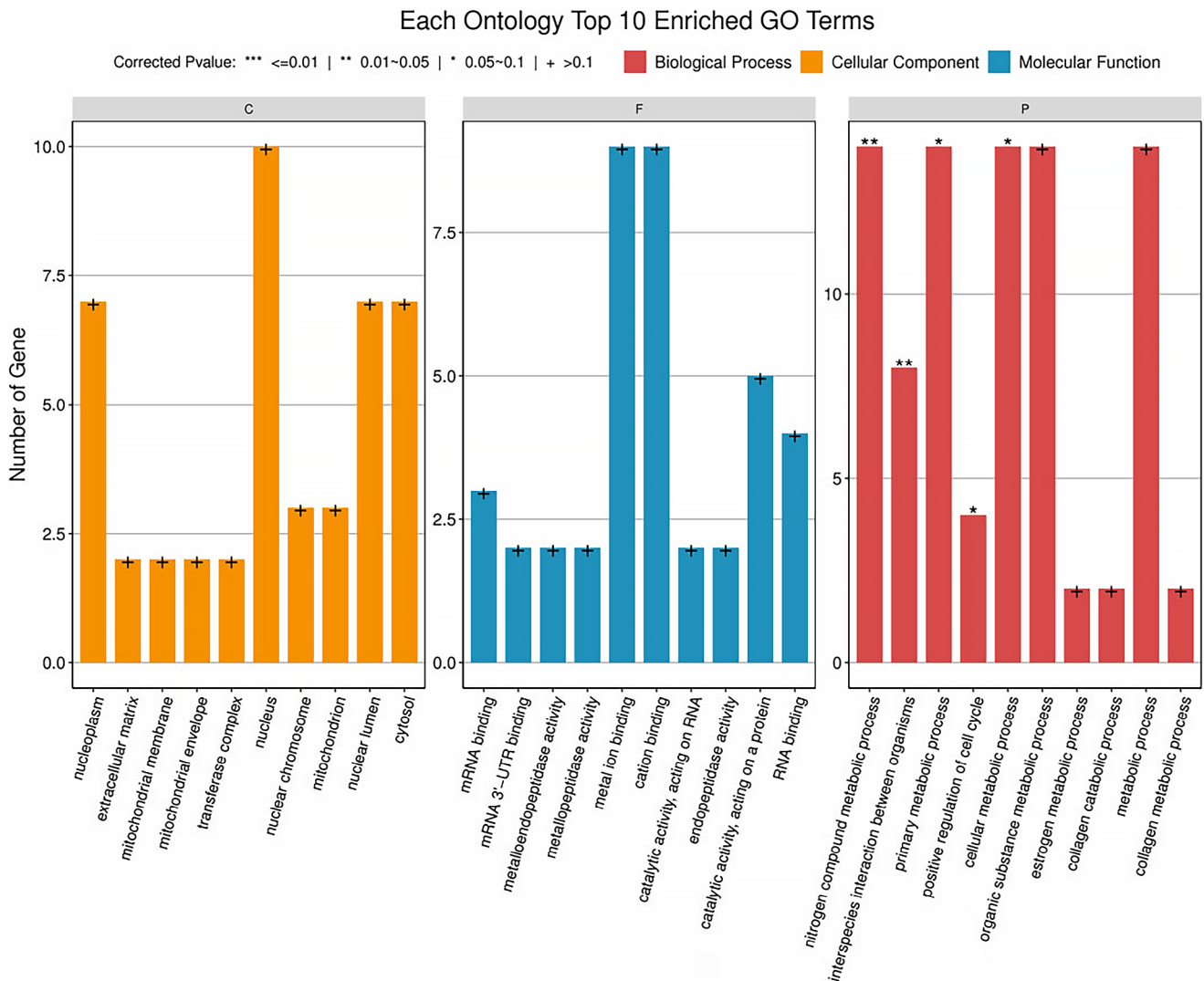


Fig. 4. Gene Ontology (GO) analysis of differentially expressed (DE) mRNAs. GO analysis showing biological process (green points), cellular component (purple points), and molecular function (orange points). The x-axis represents the number of DE mRNAs, and the y-axis lists the pathway names

metal ion binding. The enriched KEGG pathways included the IL-17 signaling pathway, the peroxisome proliferator-activated receptors (PPAR) signaling pathway, tryptophan metabolism, and the metabolism of xenobiotics by cytochrome P450. Interleukin 17 is considered to play a role in regulating corneal inflammatory responses,⁵⁹ and the PPAR signaling pathway is thought to be involved in oxidative stress and autophagy.⁶⁰

These enriched pathways, particularly IL-17 and PPAR signaling, further underscore the mechanistic links between PM_{2.5} exposure and oxidative stress, inflammation, and autophagy in the cornea.

Limitations

There are several limitations to this study. First, the fine particulate matter used, SRM 1648a, was not directly collected from ambient air but is a reference material. Its composition therefore differs somewhat from that of actual environmental PM. However, its

main components, such as various metals, polycyclic aromatic hydrocarbons, and polychlorinated biphenyl homologues, are similar to those typically adsorbed onto atmospheric PM. Second, the DE RNAs identified in this study require further validation. Despite these limitations, our work provides a foundational transcriptomic dataset and identifies several novel genes, pathways, and miRNA–mRNA interactions that may mediate PM_{2.5}-induced corneal damage, thereby laying the groundwork for further elucidation of the underlying damage mechanisms.

Conclusions

Through bioinformatics analysis, we have begun to elucidate genes and signaling pathways responsive to PM_{2.5}-induced damage and have constructed regulatory networks that may underlie these processes. These findings provide new insights into the impact of PM_{2.5} on ocular health

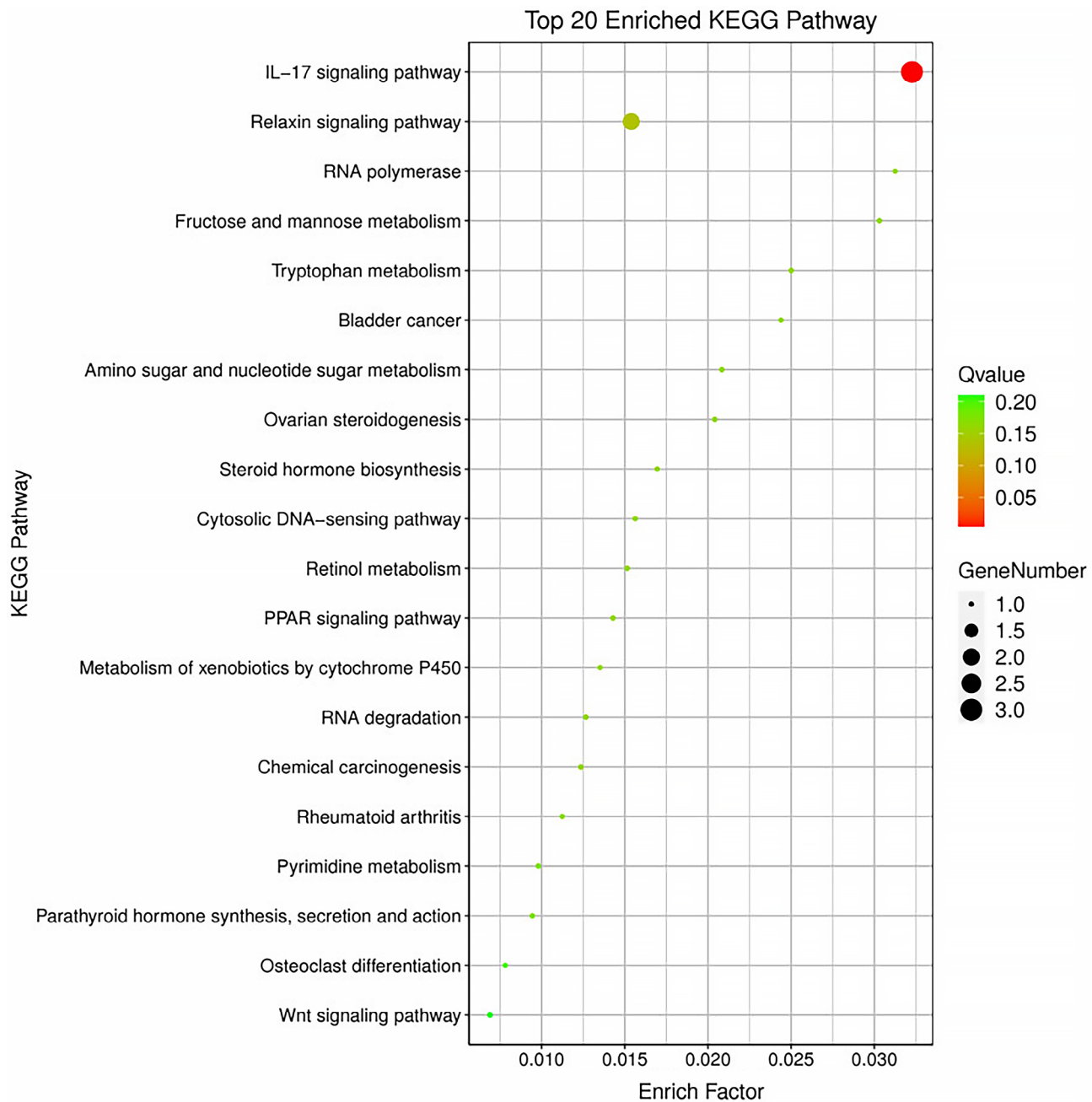


Fig. 5. Kyoto Encyclopedia of Genes and Genomes (KEGG) pathway enrichment analysis of differentially expressed (DE) mRNAs. The x-axis represents the enrichment factor, and the y-axis lists the pathway names. Dot size reflects the number of DE genes involved in each pathway. Color indicates the q value (adjusted p value), with red representing lower q values (higher statistical significance) and green representing higher q values. The top 20 enriched pathways are shown

and serve as a platform for future research in this field, potentially guiding the development of targeted diagnostics or therapies to mitigate PM_{2.5}-induced ocular surface damage.

Supplementary files

The supplementary materials are available at <https://doi.org/10.5281/zenodo.15245015>. The package contains the following files:

Supplementary Table 1. Statistical analysis data of mRNA between the NC group and the PM_{2.5} group.

Supplementary Table 2. Statistical analysis data of miRNA between the NC group and the PM_{2.5} group.

Supplementary Table 3. GO analysis of DE mRNAs.

Supplementary Table 4. KEGG signaling pathways of DE mRNAs.

Data Availability Statement

The datasets generated and analyzed during the current study are available in the NCBI repository. The accession number for these SRA data is PRJNA1233430, and its release date is June 30, 2025.

Consent for publication

Not applicable.

Use of AI and AI-assisted technologies

Not applicable.

ORCID iDs

Yingchao Li  <https://orcid.org/0000-0001-7766-9026>

Wenjing Liu  <https://orcid.org/0000-0002-4731-3552>

Huijing Bao  <https://orcid.org/0000-0001-9784-5357>

Yibin Ma  <https://orcid.org/0009-0005-5859-8206>

Han Zhang  <https://orcid.org/0000-0003-1575-0595>

References

- Manisalidis I, Stavropoulou E, Stavropoulos A, Bezirtzoglou E. Environmental and health impacts of air pollution: A review. *Front Public Health*. 2020;8:14. doi:10.3389/fpubh.2020.00014
- Thangavel P, Park D, Lee YC. Recent insights into particulate matter (PM_{2.5})-mediated toxicity in humans: An overview. *Int J Environ Res Public Health*. 2022;19(12):7511. doi:10.3390/ijerph19127511
- Wang Y, Xiao S, Zhang Y, et al. Long-term exposure to PM_{2.5} major components and mortality in the southeastern United States. *Environ Int*. 2022;158:106969. doi:10.1016/j.envint.2021.106969
- Ethan CJ, Mokoena KK, Yu Y. Air pollution status in 10 mega-cities in China during the initial phase of the COVID-19 outbreak. *Int J Environ Res Public Health*. 2021;18(6):3172. doi:10.3390/ijerph18063172
- Shi S, Wang W, Li X, et al. Evolution in disparity of PM_{2.5} pollution in China. *Eco Environ Health*. 2023;2(4):257–263. doi:10.1016/j.eehl.2023.08.007
- Basith S, Manavalan B, Shin TH, et al. The impact of fine particulate matter 2.5 on the cardiovascular system: A review of the invisible killer. *Nanomaterials*. 2022;12(15):2656. doi:10.3390/nano12152656
- Guo J, Chai G, Song X, et al. Long-term exposure to particulate matter on cardiovascular and respiratory diseases in low- and middle-income countries: A systematic review and meta-analysis. *Front Public Health*. 2023;11:1134341. doi:10.3389/fpubh.2023.1134341
- Hayes RB, Lim C, Zhang Y, et al. PM_{2.5} air pollution and cause-specific cardiovascular disease mortality. *Int J Epidemiol*. 2020;49(1):25–35. doi:10.1093/ije/dy114
- Krittawanong C, Qadeer YK, Hayes RB, et al. PM_{2.5} and cardiovascular diseases: State-of-the-art review. *Int J Cardiol Cardiovasc Risk Prev*. 2023;19:200217. doi:10.1016/j.ijcrp.2023.200217
- Moon J, Kim E, Jang H, et al. Long-term exposure to PM_{2.5} and mortality: A national health insurance cohort study. *Int J Epidemiol*. 2024;53(6):dya140. doi:10.1093/ije/dyae140
- Xiang P, Liu RY, Sun HJ, et al. Molecular mechanisms of dust-induced toxicity in human corneal epithelial cells: Water and organic extract of office and house dust. *Environ Int*. 2016;92–93:348–356. doi:10.1016/j.envint.2016.04.013
- Chen ZH, Wu YF, Wang PL, et al. Autophagy is essential for ultrafine particle-induced inflammation and mucus hyperproduction in airway epithelium. *Autophagy*. 2016;12(2):297–311. doi:10.1080/15548627.2015.1124224
- Han JH, Amri C, Lee H, Hur J. Pathological mechanisms of particulate matter-mediated ocular disorders: A review. *Int J Mol Sci*. 2024;25(22):12107. doi:10.3390/ijms252212107
- Li T, Yu Y, Sun Z, Duan J. A comprehensive understanding of ambient particulate matter and its components on the adverse health effects based from epidemiological and laboratory evidence. *Part Fibre Toxicol*. 2022;19(1):67. doi:10.1186/s12989-022-00507-5
- Yu D, Cai W, Shen T, et al. PM_{2.5} exposure increases dry eye disease risks through corneal epithelial inflammation and mitochondrial dysfunctions. *Cell Biol Toxicol*. 2023;39(6):2615–2630. doi:10.1007/s10565-023-09791-z
- Zhang K. Environmental PM_{2.5}-triggered stress responses in digestive diseases. *eGastroenterology*. 2024;2(2):e100063. doi:10.1136/egastro-2024-100063
- Meng S, Hu H, Qiao Y, et al. A versatile hydrogel with antibacterial and sequential drug-releasing capability for the programmable healing of infectious keratitis. *ACS Nano*. 2023;17(23):24055–24069. doi:10.1021/acsnano.3c09034
- Sun X, Qiao Y, Zhao L, et al. Application of decellularized porcine sclera in repairing corneal perforations and lamellar injuries. *ACS Biomater Sci Eng*. 2022;8(12):5295–5306. doi:10.1021/acsbmaterials.2c00972
- Wang F, Shi W, Li H, et al. Decellularized porcine cornea-derived hydrogels for the regeneration of epithelium and stroma in focal corneal defects. *Ocul Surf*. 2020;18(4):748–760. doi:10.1016/j.jtos.2020.07.020
- Bolger AM, Lohse M, Usadel B. Trimmomatic: A flexible trimmer for Illumina sequence data. *Bioinformatics*. 2014;30(15):2114–2120. doi:10.1093/bioinformatics/btu170
- Kim D, Langmead B, Salzberg SL. HISAT: A fast spliced aligner with low memory requirements. *Nat Methods*. 2015;12(4):357–360. doi:10.1038/nmeth.3317
- Li H, Handsaker B, Wysoker A, et al. The Sequence Alignment/Map format and SAMtools. *Bioinformatics*. 2009;25(16):2078–2079. doi:10.1093/bioinformatics/btp352
- Perteau M, Perteau GM, Antonescu CM, Chang TC, Mendell JT, Salzberg SL. StringTie enables improved reconstruction of a transcriptome from RNA-seq reads. *Nat Biotechnol*. 2015;33(3):290–295. doi:10.1038/nbt.3122
- Love MI, Huber W, Anders S. Moderated estimation of fold change and dispersion for RNA-seq data with DESeq2. *Genome Biol*. 2014;15(12):550. doi:10.1186/s13059-014-0550-8
- Yu G, Li F, Qin Y, Bo X, Wu Y, Wang S. GOSemSim: An R package for measuring semantic similarity among GO terms and gene products. *Bioinformatics*. 2010;26(7):976–978. doi:10.1093/bioinformatics/btq064
- Li B, Ma Y, Zhou Y, Chai E. Research progress of different components of PM_{2.5} and ischemic stroke. *Sci Rep*. 2023;13(1):15965. doi:10.1038/s41598-023-43119-5
- Lu X, Zhang H, Wang M, et al. Novel insights into the role of BRD4 in fine particulate matter induced airway hyperresponsiveness. *Ecotoxicol Environ Saf*. 2021;221:112440. doi:10.1016/j.ecoenv.2021.112440
- Zhang GZ, Chen HW, Deng Y jun, et al. BRD4 inhibition suppresses senescence and apoptosis of nucleus pulposus cells by inducing autophagy during intervertebral disc degeneration: An in vitro and in vivo study. *Oxid Med Cell Longev*. 2022;2022(1):9181412. doi:10.1155/2022/9181412
- Gong ZG, Zhao Y, Wang ZY, Fan RF, Liu ZP, Wang L. Epigenetic regulator BRD4 is involved in cadmium-induced acute kidney injury via contributing to lysosomal dysfunction, autophagy blockade and oxidative stress. *J Hazard Mater*. 2022;423:127110. doi:10.1016/j.jhazmat.2021.127110
- Liu H, Wang L, Weng X, et al. Inhibition of Brd4 alleviates renal ischemia/reperfusion injury-induced apoptosis and endoplasmic reticulum stress by blocking FoxO4-mediated oxidative stress. *Redox Biol*. 2019;24:101195. doi:10.1016/j.redox.2019.101195
- De Noon S, Piggott R, Trotman J, et al. Recurrent FOSL1 rearrangements in desmoplastic fibroblastoma. *J Pathol*. 2023;259(2):119–124. doi:10.1002/path.6038
- Zhai X, Wang J, Sun J, Xin L. PM_{2.5} induces inflammatory responses via oxidative stress-mediated mitophagy in human bronchial epithelial cells. *Toxicol Res*. 2022;11(1):195–205. doi:10.1093/toxres/tfac001
- Zhong L, Fang S, Wang AQ, et al. Identification of the Fos1/AMPK/autophagy axis involved in apoptotic and inflammatory effects following spinal cord injury. *Int Immunopharmacol*. 2022;103:108492. doi:10.1016/j.intimp.2021.108492
- Niidome K, Taniguchi R, Yamazaki T, Tsuji M, Itoh K, Ishihara Y. FosL1 is a novel target of levetiracetam for suppressing the microglial inflammatory reaction. *Int J Mol Sci*. 2021;22(20):10962. doi:10.3390/ijms222010962
- Liang Y, Han D, Zhang S, Sun L. FOSL1 regulates hyperproliferation and NLRP3-mediated inflammation of psoriatic keratinocytes through the NF-κB signaling via transcriptionally activating TRAF3. *Biochim Biophys Acta Mol Cell Res*. 2024;1871(5):119689. doi:10.1016/j.bbamcr.2024.119689
- Li N, Zhan X. Machine learning identifies pan-cancer landscape of Nrf2 oxidative stress response pathway-related genes. *Oxid Med Cell Longev*. 2022;2022(1):8450087. doi:10.1155/2022/8450087

37. Bathish B, Robertson H, Dillon JF, Dinkova-Kostova AT, Hayes JD. Nonalcoholic steatohepatitis and mechanisms by which it is ameliorated by activation of the CNC-bZIP transcription factor Nrf2. *Free Radic Biol Med.* 2022;188:221–261. doi:10.1016/j.freeradbiomed.2022.06.226
38. Guo S, Ramar V, Guo AA, et al. TRPM7 transactivates the *FOSL1* gene through STAT3 and enhances glioma stemness. *Cell Mol Life Sci.* 2023; 80(9):270. doi:10.1007/s00018-023-04921-6
39. Zhang C, Wang X, Pi S, et al. Cadmium and molybdenum co-exposure triggers autophagy via CYP450s/ROS pathway in duck renal tubular epithelial cells. *Sci Total Environ.* 2021;759:143570. doi:10.1016/j.scitotenv.2020.143570
40. Coelho NR, Pimpão AB, Correia MJ, et al. Pharmacological blockade of the AHR-CYP1A1 axis: A call for in vivo evidence. *J Mol Med.* 2022;100(2):215–243. doi:10.1007/s00109-021-02163-2
41. Yuan J, Sun X, Che S, et al. AhR-mediated CYP1A1 and ROS overexpression are involved in hepatotoxicity of decabromodiphenyl ether (BDE-209). *Toxicol Lett.* 2021;352:26–33. doi:10.1016/j.toxlet.2021.09.008
42. Song Y, Yen S, Southam K, Gaskin S, Hoy RF, Zosky GR. The aryl hydrocarbon receptor pathway is a marker of lung cell activation but does not play a central pathologic role in engineered stone-associated silicosis. *J Appl Toxicol.* 2024;44(10):1518–1527. doi:10.1002/jat.4653
43. Zhan Y, Zhang Z, Liu Y, et al. NUPR1 contributes to radiation resistance by maintaining ROS homeostasis via AhR/CYP signal axis in hepatocellular carcinoma. *BMC Med.* 2022;20(1):365. doi:10.1186/s12916-022-02554-3
44. Alluli A, Fonseca G, Matthews J, Eidelman DH, Baglolle CJ. Regulation of long non-coding RNA expression by aryl hydrocarbon receptor activation. *Toxicol Lett.* 2024;391:13–25. doi:10.1016/j.toxlet.2023.11.004
45. Zhang Y, Song M, Bi Y, Lei Y, Sun X, Chen Y. TIPARP is involved in the regulation of intraocular pressure. *Commun Biol.* 2022;5(1):1386. doi:10.1038/s42003-022-04346-0
46. Liang G, Ling Y, Mehrpour M, et al. Autophagy-associated circRNA circCDYL augments autophagy and promotes breast cancer progression. *Mol Cancer.* 2020;19(1):65. doi:10.1186/s12943-020-01152-2
47. Jin Q, Ma X, Wang G, Yang X, Guo F. Dynamics of major air pollutants from crop residue burning in mainland China, 2000–2014. *J Environ Sci.* 2018;70:190–205. doi:10.1016/j.jes.2017.11.024
48. Zeng Z, Ma H, Chen J, et al. Knockdown of miR-1275 protects against cardiomyocytes injury through promoting neuromedin U type 1 receptor. *Cell Cycle.* 2020;19(24):3639–3649. doi:10.1080/15384101.2020.1860310
49. Zhang DM, Deng JJ, Wu YG, et al. MicroRNA-223-3p protect against radiation-induced cardiac toxicity by alleviating myocardial oxidative stress and programmed cell death via targeting the AMPK pathway. *Front Cell Dev Biol.* 2022;9:801661. doi:10.3389/fcell.2021.801661
50. Fernando N, Wong JHC, Das S, et al. MicroRNA-223 regulates retinal function and inflammation in the healthy and degenerating retina. *Front Cell Dev Biol.* 2020;8:516. doi:10.3389/fcell.2020.00516
51. Tang H, Lin Y, Huang L, Hu J. MiR-223-3p regulates autophagy and inflammation by targeting ATG16L1 in *Fusarium solani*-induced keratitis. *Invest Ophthalmol Vis Sci.* 2022;63(1):41. doi:10.1167/iovs.63.1.41
52. Lv P, Liu H, Ye T, et al. XIST inhibition attenuates calcium oxalate nephrocalcinosis-induced renal inflammation and oxidative injury via the miR-223/NLRP3 pathway. *Oxid Med Cell Longev.* 2021;2021(1):1676152. doi:10.1155/2021/1676152
53. Chang Q, Ji M, Li C, Geng R. Downregulation of miR-486-5p alleviates LPS-induced inflammatory injury, oxidative stress and apoptosis in chondrogenic cell ATDC5 by targeting NRF1. *Mol Med Rep.* 2020;22(3):2123–2131. doi:10.3892/mmr.2020.11289
54. Ma N, Li S, Lin C, Cheng X, Meng Z. Mesenchymal stem cell conditioned medium attenuates oxidative stress injury in hepatocytes partly by regulating the miR-486-5p/PIM1 axis and the TGF- β /Smad pathway. *Bioengineered.* 2021;12(1):6434–6447. doi:10.1080/21655979.2021.1972196
55. Yongprayoon V, Wattanakul N, Khomate W, et al. Targeting BRD4: Potential therapeutic strategy for head and neck squamous cell carcinoma (Review). *Oncol Rep.* 2024;51(6):74. doi:10.3892/or.2024.8733
56. Li X, Lv Y, Hao J, et al. Role of microRNA-4516 involved autophagy associated with exposure to fine particulate matter. *Oncotarget.* 2016;7(29):45385–45397. doi:10.18632/oncotarget.9978
57. Mancini FR, Laine JE, Tarallo S, et al. microRNA expression profiles and personal monitoring of exposure to particulate matter. *Environ Pollut.* 2020;263:114392. doi:10.1016/j.envpol.2020.114392
58. Cao Y, Li P, Zhang G, et al. MicroRNA Let-7c-5p-mediated regulation of ERCC6 disrupts autophagic flux in age-related cataract via the binding to VCP. *Curr Eye Res.* 2021;46(9):1353–1362. doi:10.1080/02713683.2021.1900273
59. Xue Y, Xu P, Hu Y, et al. Stress systems exacerbate the inflammatory response after corneal abrasion in sleep-deprived mice via the IL-17 signaling pathway. *Mucosal Immunol.* 2024;17(3):323–345. doi:10.1016/j.mucimm.2024.02.009
60. Muzio G, Barrera G, Pizzimenti S. Peroxisome proliferator-activated receptors (PPARs) and oxidative stress in physiological conditions and in cancer. *Antioxidants (Basel).* 2021;10(11):1734. doi:10.3390/antiox10111734